Joint International Topical Meeting on Mathematics & Computation and Supercomputing in Nuclear Applications (M&C + SNA 2007)
Monterey, California, April 15-19, 2007, on CD-ROM, American Nuclear Society, LaGrange Park, IL (2007)

A HYBRID MONTE CARLO-DIFFUSION METHOD FOR RADIATION TRANSPORT ON ADAPTIVE MESH REFINEMENT-TYPE MESHES

Jeffery D. Densmore, Thomas M. Evans, and Michael W. Buksas
Computational Physics and Methods Group, Los Alamos National Laboratory
P.O. Box 1663, MS D409, Los Alamos, NM 87545, USA
jdd@lanl.gov; tme@lanl.gov; mwbuksas@lanl.gov

ABSTRACT

Discrete Diffusion Monte Carlo (DDMC) is a technique for increasing the efficiency of Monte Carlo simulations in diffusive media. We present a new DDMC method for linear, steady-state, radiation transport on Adaptive Mesh Refinement (AMR) meshes in two-dimensional Cartesian geometry. We specifically examine the cases of (i) a regular mesh structure without refinement, (ii) a refined mesh structure where neighboring cells differ in refinement, and (iii) a boundary mesh structure at the interface between a diffusive region (where DDMC is used) and a non-diffusive region (where standard Monte Carlo is employed). With a test problem consisting of both diffusive and non-diffusive regions, we demonstrate that our new DDMC technique is more computationally efficient than standard Monte Carlo while still producing accurate solutions.

Key Words: Hybrid Monte Carlo-diffusion; Adaptive mesh refinement

1. INTRODUCTION

Discrete Diffusion Monte Carlo (DDMC) is a technique for increasing the efficiency of Monte Carlo radiation-transport simulations in diffusive media [1–6]. This type of media is characterized by a small mean-free path and collisions that are primarily scattering events. A standard Monte Carlo simulation in this regime consists of extremely long particle histories due to the small distance between collisions and lack of absorption, a situation that results in a computationally inefficient calculation. In DDMC, particles take discrete steps between spatial cells according to a discretized diffusion equation. Since each DDMC step replaces many small Monte Carlo steps, DDMC should be more efficient than standard Monte Carlo in diffusive media. In addition, given that DDMC is based on diffusion theory, DDMC should produce accurate solutions if used judiciously. In practice, DDMC is combined with standard Monte Carlo to form a hybrid method that can treat problems with both diffusive and non-diffusive regions.

In this paper, we present a DDMC method for linear, steady-state, radiation transport on Adaptive Mesh Refinement (AMR) meshes in two-dimensional Cartesian geometry [5]. This type of mesh is characterized by local refinement such that spatial cells may have multiple neighboring cells across each face and is commonly employed in Eulerian hydrodynamics calculations [7, 8]. Although we examine a simplified problem, our ultimate goal is to extend the methodology developed here to coupled radiation-hydrodynamics simulations [9]. Developing a DDMC method for AMR meshes is important for these types of calculations for two reasons. First, diffusive regions arise in such problems due to the linearization of the underlying nonlinear, time-dependent, radiation-transport process [10]. Second, if an AMR mesh is employed in the hydrodynamics portion of the simulation, then a DDMC technique amenable to this type of mesh must be used for the corresponding radiation-transport calculation.

We begin the remainder of this paper by developing our DDMC method for AMR meshes. We specifically examine the cases of (i) a regular mesh structure without refinement, (ii) a refined mesh structure where neighboring cells differ in refinement, and (iii) a boundary mesh structure representing the interface between diffusive and non-diffusive regions. The treatment of a boundary mesh structure demonstrates how to couple DDMC to standard Monte Carlo. With a test problem consisting of both diffusive and non-diffusive regions, we compare our new DDMC technique to both standard Monte Carlo and Random Walk (RW) [11, 12], another hybrid method for increasing the efficiency of Monte Carlo simulations in diffusive media. We conclude with a brief discussion summarizing our new DDMC technique and outlining areas for future work.

2. DEVELOPMENT OF DDMC EQUATIONS

We begin by considering the following steady-state, monoenergetic, diffusion equation [13]:

$$-\boldsymbol{\nabla}\cdot\frac{1}{3\Sigma_t}\boldsymbol{\nabla}\phi+\Sigma_a\phi=Q \quad . \tag{1}$$

Here, $\phi(\mathbf{r})$ is the scalar flux, $\Sigma_t(\mathbf{r})$ is the total cross section, $\Sigma_a(\mathbf{r})$ is the absorption cross section, $Q(\mathbf{r})$ is the radiation source, and $\mathbf{r}=x\mathbf{i}+y\mathbf{j}$ is the spatial variable in two-dimensional Cartesian geometry. We assume that Eq. (1) is valid in some problem subdomain that has been designated for simulation by DDMC and that standard Monte Carlo is employed in the remainder of the problem. In order to couple DDMC and and standard Monte Carlo, we employ the asymptotic diffusion-limit boundary condition. At a point $\mathbf{r}$ on the boundary of the DDMC region, this boundary condition is given by [14]

$$2\int_{\boldsymbol{\Omega}\cdot\mathbf{n}<0}W(|\boldsymbol{\Omega}\cdot\mathbf{n}|)\psi_b(\mathbf{r},\boldsymbol{\Omega})d\boldsymbol{\Omega}=\phi+\frac{d}{\Sigma_t}\mathbf{n}\cdot\boldsymbol{\nabla}\phi \quad . \tag{2}$$

Here, $\psi_b(\mathbf{r},\boldsymbol{\Omega})$ is the angular flux incident on the boundary of the DDMC region in direction $\boldsymbol{\Omega}$ due to a simultaneous Monte Carlo simulation, $d\approx 0.7104$ is the *extrapolation distance*, and $\mathbf{n}$ is the the unit-outward normal vector on the boundary. In addition, $W(\mu)$ is a transcendental function well approximated by

$$W(\mu)\approx 0.91\mu+1.635\mu^2 \quad . \tag{3}$$

Our DDMC method is developed by discretizing Eqs. (1) and (2) on an AMR mesh. We adapt the work of Edwards [15] and Olson and Morel [16] by giving the resulting finite-difference equations a Monte Carlo interpretation. This discretization has the desirable properties that it (i) converges as the mesh size is refined and (ii) preserves linear solutions. The specific type of AMR mesh our DDMC technique employs consists of orthogonal cells with the following properties [8]:

- The lowest-level (i.e., coarsest level) mesh is uniform with a mesh spacing of Δx and Δy.
- Higher-level (i.e., finer-level) meshes are constructed by dividing the mesh spacing of the lowest-level mesh by factors of two.
- Neighboring cells may only differ by one level of refinement such that each cell may have a maximum of two neighbors on each face.

2.1. Regular Mesh Structure

We first examine a regular mesh structure without refinement as illustrated in Fig. 1. We will present the DDMC equation corresponding to cell 3, although the equations for other cells can be developed in a similar manner. Using a standard finite-difference discretization of Eq. (1) [15, 16] and rearranging terms shows the DDMC equation for cell 3 to be

$$\left(\Sigma_{3\to2}+\Sigma_{3\to5}+\Sigma_{3\to4}+\Sigma_{3\to1}+\Sigma_{a,3}\right)\phi_3 = Q_3+\frac{1}{\Delta x\Delta y}\left(\Sigma_{2\to3}\phi_2+\Sigma_{5\to3}\phi_5+\Sigma_{4\to3}\phi_4+\Sigma_{1\to3}\phi_1\right)\Delta x\Delta y \quad . \quad (4)$$

Here, we have defined the leakage cross sections as

$$\Sigma_{3\to2}=\Sigma_{2\to3}=\left(\frac{1}{\Delta y}\right)^2\frac{2}{3(\Sigma_{t,3}+\Sigma_{t,2})} \quad , \quad (5)$$

$$\Sigma_{3\to5}=\Sigma_{5\to3}=\left(\frac{1}{\Delta x}\right)^2\frac{2}{3(\Sigma_{t,3}+\Sigma_{t,5})} \quad , \quad (6)$$

$$\Sigma_{3\to4}=\Sigma_{4\to3}=\left(\frac{1}{\Delta y}\right)^2\frac{2}{3(\Sigma_{t,3}+\Sigma_{t,4})} \quad , \quad (7)$$

and

$$\Sigma_{3\to1}=\Sigma_{1\to3}=\left(\frac{1}{\Delta x}\right)^2\frac{2}{3(\Sigma_{t,3}+\Sigma_{t,1})} \quad . \quad (8)$$

In Eqs. (5)–(8), we have used appropriate cell-averaged values for the scalar flux, cross sections, and radiation source.

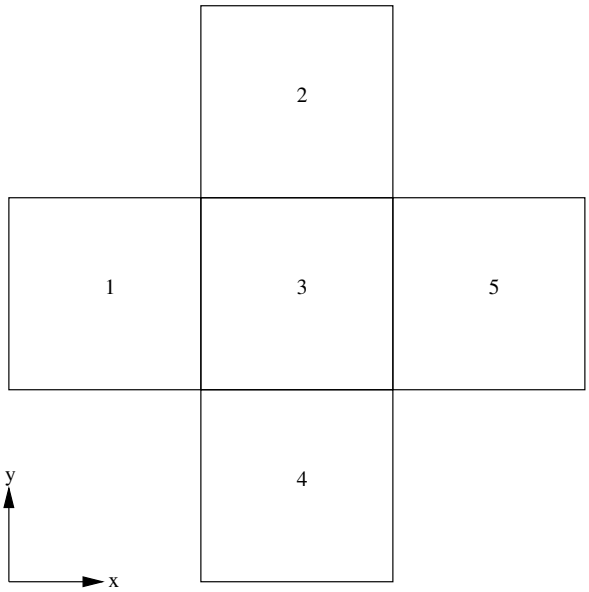

Figure 1. Regular Mesh Structure

We now give Eq. (4) a Monte Carlo interpretation. This equation can be viewed as an infinite-medium transport problem for a given cell. From the left side of Eq. (4), particles can undergo leakage reactions to

neighboring cells or be absorbed. The right side of Eq. (4) contains not only the usual radiation source term but also source terms corresponding to particles experiencing leakage reactions in neighboring cells. These leakage source terms can be interpreted as the total rate at which particles undergo leakage reactions in adjacent cells (i.e., the leakage cross section multiplied by the cell-averaged scalar flux multiplied by the the cell volume) divided by the volume of the current cell such that leaked particles are distributed evenly over the cell.

2.2. Refined Mesh Structure

Next, we consider the case where neighboring cells differ by one level of refinement. An example of this type of mesh is given in Fig. 2. To demonstrate our DDMC methodology, we develop discretized versions of Eq. (1) for for cells 3 and 7. We note that cell 7 is one level of refinement higher than cell 3, and the refined mesh spacing is $\Delta x/2$ and $\Delta y/2$.

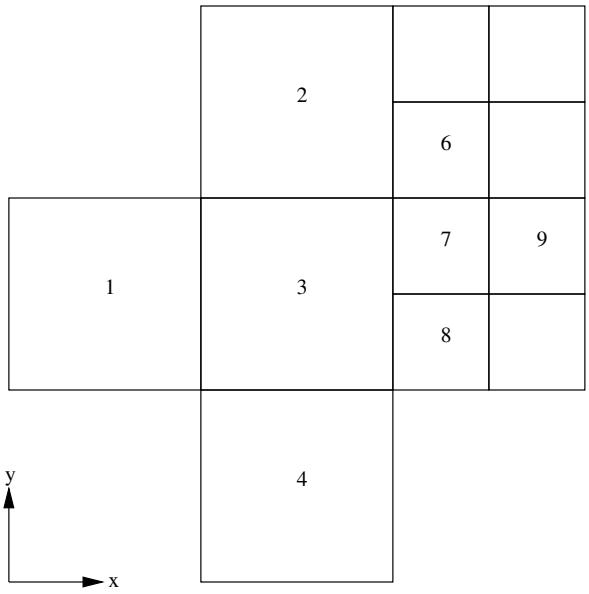

Figure 2. Refined Mesh Structure

Analogous to the derivation of Eq. (4), a finite-difference approximation of Eq. (1) for cell 3 [15, 16] and a rearrangement of terms yields

$$\left(\Sigma_{3\to2}+\Sigma_{3\to7}+\Sigma_{3\to8}+\Sigma_{3\to4}+\Sigma_{3\to1}+\Sigma_{a,3}\right)\phi_3 = Q_3+\frac{1}{\Delta x\Delta y}\left(\Sigma_{2\to3}\phi_2+\Sigma_{4\to3}\phi_4+\Sigma_{1\to3}\phi_1\right)\Delta x\Delta y+\frac{1}{\Delta x\Delta y}\left(\Sigma_{7\to3}\phi_7+\Sigma_{8\to3}\phi_8\right)\frac{\Delta x\Delta y}{4} \quad . \quad (9)$$

In addition to the leakage cross sections given by Eqs. (5), (7), and (8), we have defined the leakage cross sections between the two refinement levels as

$$\Sigma_{3\to7}=\Sigma_{3\to8}=\left(\frac{1}{\Delta x}\right)^2\frac{4}{3(4\Sigma_{t,3}+\Sigma_{t,7}+\Sigma_{t,8})} \quad , \quad (10)$$

and

$$\Sigma_{7\to3}=\Sigma_{8\to3}=\left(\frac{2}{\Delta x}\right)^2\frac{4}{3(4\Sigma_{t,3}+\Sigma_{t,7}+\Sigma_{t,8})} \quad . \quad (11)$$

Also, the DDMC equation corresponding to cell 7 is

$$\left(\Sigma_{7\to6}+\Sigma_{7\to9}+\Sigma_{7\to8}+\Sigma_{7\to3}+\Sigma_{a,7}\right)\phi_7 = Q_7+\frac{4}{\Delta x\Delta y}\left(\Sigma_{6\to7}\phi_6+\Sigma_{9\to7}\phi_9+\Sigma_{8\to7}\phi_8\right)\frac{\Delta x\Delta y}{4}+\frac{4}{\Delta x\Delta y}\Sigma_{3\to7}\phi_3\Delta x\Delta y \quad . \quad (12)$$

Here, the leakage cross sections on the refined mesh are given by

$$\Sigma_{7\to6}=\Sigma_{6\to7}=\left(\frac{2}{\Delta y}\right)^2\frac{2}{3(\Sigma_{t,7}+\Sigma_{t,8})} \quad , \quad (13)$$

$$\Sigma_{7\to9}=\Sigma_{9\to7}=\left(\frac{2}{\Delta x}\right)^2\frac{2}{3(\Sigma_{t,7}+\Sigma_{t,9})} \quad , \quad (14)$$

and

$$\Sigma_{7\to8}=\Sigma_{8\to7}=\left(\frac{2}{\Delta y}\right)^2\frac{2}{3(\Sigma_{t,7}+\Sigma_{t,8})}-\left(\frac{2}{\Delta x}\right)^2\frac{2}{3(4\Sigma_{t,3}+\Sigma_{t,7}+\Sigma_{t,8})} \quad . \quad (15)$$

Equations (9) and (12) are amenable to Monte Carlo simulation in the same manner as Eq. (4). Note the extra coefficients of four and one-fourth on some of the leakage source terms in these equations. These coefficients are due to the factor of four difference in cell volume between refinement levels. One difficulty in a Monte Carlo simulations of Eq. (12) is that it is possible for the leakage cross section given by Eq. (15) to be negative. This undesirable situation is avoided if

$$\left(\frac{\Delta y}{\Delta x}\right)^2\le\frac{4\Sigma_{t,3}+\Sigma_{t,7}+\Sigma_{t,8}}{\Sigma_{t,7}+\Sigma_{t,8}} \quad . \quad (16)$$

Equation (16) is always satisfied for meshes with an aspect ratio of unity (i.e., $\Delta x=\Delta y$) [15].

2.3. Boundary Mesh Structure

Finally, we examine the boundary of a DDMC region, as depicted in Fig. 3. We assume that an angular flux is incident on the left face of cell 3 due to a simultaneous Monte Carlo simulation in the neighboring non-diffusive region.

To develop a DDMC equation for cell 3, we employ the asymptotic interface method [17, 18]. This interface technique determines how to convert Monte Carlo particles incident on the boundary of the DDMC region into DDMC particles and how to convert DDMC particles that leave a DDMC region into Monte Carlo particles. As its name implies, this interface method is based on the asymptotic diffusion-limit boundary condition given by Eq. (2). The asymptotic interface method has the desirable property that it can produce accurate solutions in the interior of DDMC regions regardless of the angular distribution of incident Monte Carlo particles.

Discretizing Eqs. (1) and (2) shows the DDMC equation for cell 3 to be

$$\left(\Sigma_{3\to2}+\Sigma_{3\to5}+\Sigma_{3\to4}+\Sigma_{3\to b}+\Sigma_{a,3}\right)\phi_3 = Q_3+\frac{1}{\Delta x\Delta y}\left(\Sigma_{2\to3}\phi_2+\Sigma_{5\to3}\phi_5+\Sigma_{4\to3}\phi_4\right)\Delta x\Delta y + \frac{1}{\Delta x\Delta y}\int_{\partial V_{3,b}}\int_{\mathbf{\Omega}\cdot\mathbf{n}<0}P(|\mathbf{\Omega}\cdot\mathbf{n}|)|\mathbf{\Omega}\cdot\mathbf{n}|\psi_b(\mathbf{r},\mathbf{\Omega})d\mathbf{\Omega}dS \quad . \quad (17)$$

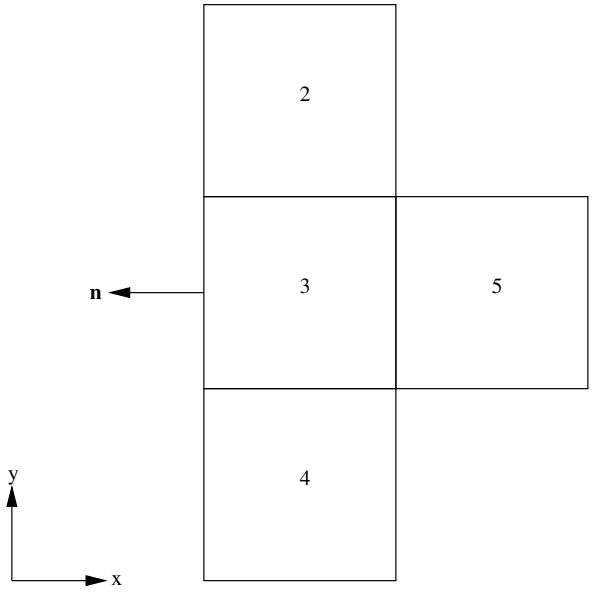

Figure 3. Boundary Mesh Structure

Here, $\partial V_{3,b}$ is the left face of cell 3 and $\mathbf{n} = -\mathbf{i}$ is the unit-outward normal vector on this face. In addition, we have defined the leakage cross section $\Sigma_{3\rightarrow b}$ as

$$\Sigma_{3\rightarrow b} = \frac{1}{\Delta x}\frac{2}{3\Sigma_{t,3}\Delta x + 6d} \quad , \tag{18}$$

and the conversion probability to be

$$P(\mu) = \frac{4}{3\Sigma_{t,3}\Delta x + 6d}\left(0.91 + 1.635\mu\right) \quad . \tag{19}$$

Equation (17) has a Monte Carlo interpretation similar to that of Eq. (4). The only difference on the left side is a leakage cross section corresponding to DDMC particles leaving the DDMC region through the left face of cell 3. On the right side there is now a source term due to Monte Carlo particles incident on the boundary of the DDMC region. This source term corresponds to the rate at which radiation is incident on the cell face in a given direction times the conversion probability given by Eq. (19), integrated over all incident directions. Thus, we can sample Eq. (19) to determine if an incident Monte Carlo particle is converted into a DDMC particle. If a particle is converted, it begins transporting via DDMC in cell 3. Otherwise, the particle is placed on the boundary of the DDMC region and continues transporting according to standard Monte Carlo in the adjacent non-diffusive region. The directions of Monte Carlo particles not converted into DDMC particles and DDMC particles that that leave the DDMC region can be sampled using techniques given by Davidson *et al.* [19].

3. NUMERICAL RESULTS

We now demonstrate the accuracy and increased efficiency, with respect to standard Monte Carlo and RW, of our new DDMC method for AMR meshes with a test problem consisting of both diffusive and non-diffusive regions. This problem features a purely scattering region with an embedded duct. The duct is

void and has a dogleg midway through the purely scattering region. The geometry of this test problem is depicted in Fig. 4. In Regions I and III, Σ_t = 100 cm^{-1}, Σ_a = 0 cm^{-1}, and Q = 0 cm^{-3}-s^{-1}, while in Region II, Σ_t = 0 cm^{-1}, Σ_a = 0 cm^{-1}, and Q = 0 cm^{-3}-s^{-1}. An isotropic incident flux is prescribed at the entrance of the duct (10 cm $\leq x \leq$ 15 cm, y = 0 cm) with an incoming current of 1 cm^{-2}-s^{-1}. All other boundaries are vacuum.

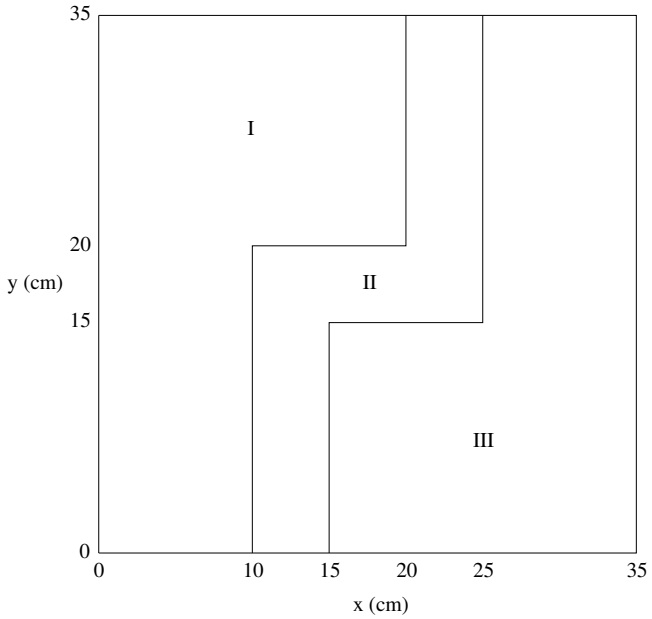

Figure 4. Problem Geometry

The computational mesh for this problem is illustrated in Fig. 5. Note that this mesh has three different levels of refinement, a unit aspect ratio, and cell sizes ranging from 2.5 cm (250 mean-free paths) to 0.625 cm (62.5 mean-free paths). We simulated this problem using standard Monte Carlo, RW, and a hybrid method consisting of standard Monte Carlo in the duct and DDMC in the purely scattering region. All three simulations only use standard Monte Carlo in the duct; the only purpose of a grid in this region is to collect scalar flux estimates. The purely scattering region has three different grid sizes, and thus this problem will test the ability of our new DDMC method to handle an AMR mesh. In each simulation, we use 10 million particles.

As stated previously, RW is another hybrid method for increasing the efficiency of Monte Carlo simulations in diffusive media [11, 12]. In RW, particles take macrosteps over spheres centered about their current positions. The radius of a RW sphere is chosen such that the sphere fits inside the particle's current spatial cell, and the macrostep is governed by an analytic solution to the diffusion equation within the sphere. In order to ensure the accuracy of the diffusion solution, the RW sphere radius (as measured in mean-free paths) is required to be larger than a specified minimum radius λ. If this minimum-radius criteria is not satisfied, RW is disabled and the particle transports according to standard Monte Carlo (for this reason, only standard Monte Carlo is used in the duct during the RW simulations). We note that, although the analytic diffusion solution is more accurate for larger spheres, RW will be invoked more often if λ is decreased. Thus, choosing a large value of λ will lead to a more accurate simulation at the expense of efficiency. In contrast, a smaller value of λ will improved efficiency while decreasing accuracy. In the calculations presented in this paper, we use two versions of RW; one with a minimum sphere radius of λ = 5 and one with a minimum sphere radius of λ = 20.

The scalar flux resulting from these simulations is plotted in Figs. 6–8. These figures give the scalar flux as a function of x for three values of y. The first value (y = 10.3125 cm) corresponds to a row of cells midway down the first leg of the duct, the second value (y = 15.3125 cm) corresponds to the row of cells just after the duct makes a turn to the right, and the third value (y = 20.3125 cm) corresponds to the row of cells just after the duct makes a turn to the left. From these figures, we see that the hybrid Monte Carlo-DDMC and RW with $\lambda = 20$ solutions agree well with the standard Monte Carlo results, while the scalar flux calculated by RW using $\lambda = 5$ is systematically too low. In particular, it appears that RW with $\lambda = 5$ does not capture the boundary layer on the right side of the duct (the small increase in the scalar flux) as seen in Figs. 7 and 8. This result is surprising, since the conventional wisdom is that RW should be able to capture boundary-layer effects because RW is disabled near cells faces (since the sphere radius is too small) and particles transport according to standard Monte Carlo. It is also interesting to note that the agreement between the hybrid and standard Monte Carlo calculations is quite good at x = 25 cm in Fig. 7. This agreement is impressive, since the geometry in this corner of the duct is two-dimensional, while the asymptotic interface method and the corresponding boundary condition given by Eq. (2) are based on a one-dimensional analysis.

In addition to yielding accurate solutions, the hybrid Monte Carlo-DDMC simulation provides a greater efficiency increase than RW over standard Monte Carlo. For this problem, the hybrid calculation was 484 times faster than standard Monte Carlo, while the RW calculation using $\lambda = 5$ was only 4 times faster than standard Monte Carlo. The RW calculation with $\lambda = 20$, although accurate, was even less efficient than the $\lambda = 5$ simulation; it was only 1.44 times faster than standard Monte Carlo.

4. CONCLUSIONS

We have presented a new DDMC method for linear, steady-state, radiation transport on AMR meshes in two-dimensional Cartesian geometry. We have specifically examined the cases of (i) a regular mesh structure without refinement, (ii) a refined mesh structure where neighboring cells differ in refinement, and (iii) a boundary mesh structure representing the interface between diffusive and non-diffusive regions. The treatment of a boundary mesh structure determines how to couple DDMC, a technique used in diffusive regions, to standard Monte Carlo, a method employed in the remainder of the problem domain.

With a test problem consisting of both diffusive and non-diffusive regions, we have demonstrated the improved efficiency of our new DDMC technique with respect to both standard Monte Carlo and RW. Specifically, we observed the hybrid Monte Carlo-DDMC calculation to be two order of magnitude faster than standard Monte Carlo, while RW outperformed standard Monte Carlo by at most a factor of four. In addition, DDMC yielded scalar fluxes that agreed well with standard Monte Carlo solutions. In contrast, RW results could be quite erroneous unless the minimum sphere radius was chosen to be sufficiently large, a situation that further decreased the efficiency of RW.

We stated in the introduction of this paper that our ultimate goal is to apply this new DDMC method for AMR meshes to coupled radiation-hydrodynamics calculations. To meet this goal, several issues remain for future work. First, we must develop a technique for automatically determining which problem regions to simulate with DDMC without user intervention. In the test problem presented in this paper, we selected *a priori* the regions to employ DDMC in, a liberty that is not practical in real calculations. In addition, this DDMC method must be adapted to both curvilinear (i.e., spherical and cylindrical) geometries and energy-dependent problems.

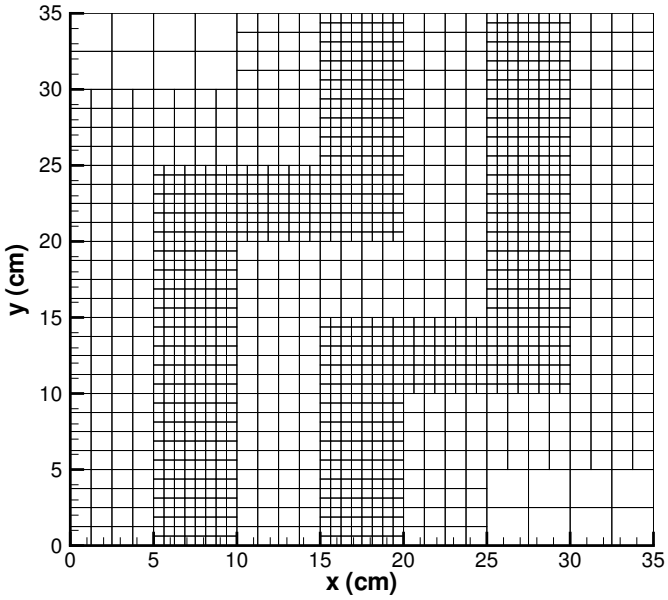

Figure 5. Computational Mesh

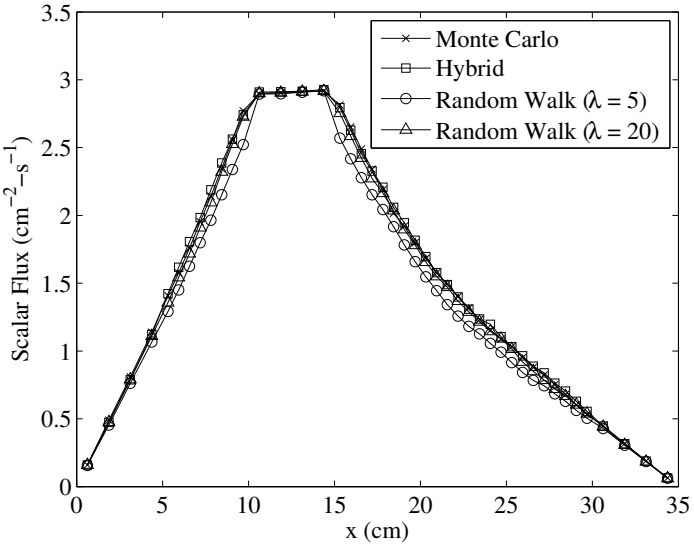

Figure 6. Scalar Flux at $y = 10.3125$ cm

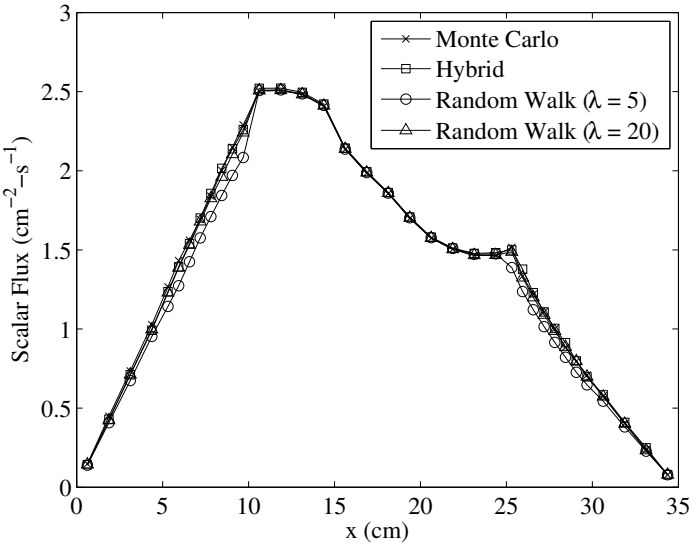

Figure 7. Scalar Flux at $y = 15.3125$ cm

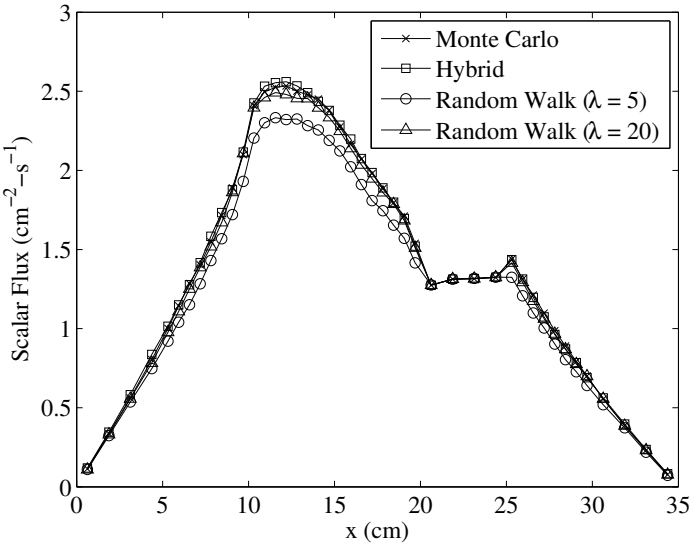

Figure 8. Scalar Flux at $y = 20.3125$ cm

ACKNOWLEDGMENTS

This work was performed under U.S. government contract DE-AC52-06NA25396 for Los Alamos National Laboratory, which is operated by Los Alamos National Security, LLC. (LANS) for the U.S. Department of Energy.

REFERENCES

[1] T.J. Urbatsch, J.E. Morel, and J.C. Gulick, "Monte Carlo Solution of Spatially-Discrete Transport Equations, Part II: Diffusion and Transport-Diffusion," *Proc. Int. Conf. Mathematics and Computation, Reactor Physics, and Environmental Analysis*, Madrid, Spain, September 27–30, 1999, Vol. 1, p. 262.

[2] T.M. Evans, T.J. Urbatsch, and H. Lichtenstein, "1-D Equilibrium Discrete Diffusion Monte Carlo," *Proc. MC2000 — International Conference*, Lisbon, Portugal, July, 2000.

[3] N.A. Gentile, "Implicit Monte Carlo Diffusion — An Acceleration Method for Monte Carlo Time-Dependent Radiative Transfer Simulations," *J. Comp. Phys.*, **172**, 543 (2001).

[4] J.D. Densmore, T.J. Urbatsch, T.M. Evans, and M.W. Buksas, "Discrete Diffusion Monte Carlo for Grey Implicit Monte Carlo Simulations," *Proc. Int. Top. Mtg. on Mathematics and Computation, Supercomputing, Reactor Physics and Nuclear and Biological Applications*, Avignon, France, September 12–15, 2005.

[5] J.D. Densmore, T.M. Evans, and M.W. Buksas, "Discrete Diffusion Monte Carlo for XY Adaptive Mesh Refinement-Style Meshes," *Trans. Am. Nucl. Soc.*, **95**, 541 (2006).

[6] J.D. Densmore, T.J. Urbatsch, T.M. Evans, and M.W. Buksas, "A Hybrid Transport-Diffusion Method for Monte Carlo Radiative-Transfer Simulations," *J. Comp. Phys.*, **222**, 485 (2007).

[7] M.J. Berger and P. Colella, "Local Adaptive Mesh Refinement for Shock Hydrodynamics," *J. Comp. Phys.*, **82**, 64 (1989).

[8] *SAGE Users Manual*, LA–UR–04–2959, Los Alamos National Laboratory (2005).

[9] D. Mihalas and B. Weibel-Mihalas, *Foundations of Radiation Hydrodynamics*, Dover Publications, Mineola, New York (1999).

[10] J.A. Fleck, Jr., and J.D. Cummings, "An Implicit Monte Carlo Scheme for Calculating Time and Frequency Dependent Nonlinear Radiation Transport," *J. Comp. Phys.*, **8**, 313 (1971).

[11] J.A. Fleck, Jr., and E.H. Canfield, "A Random Walk Procedure for Improving the Computational Efficiency of the Implicit Monte Carlo Method for Nonlinear Radiation Transport," *J. Comp. Phys.*, **54**, 508 (1984).

[12] J. Giorla and R. Sentis, "A Random Walk Method for Solving Radiative Transfer Equations," *J. Comp. Phys.*, **70**, 145 (1987).

[13] G.I. Bell and S. Glasstone, *Nuclear Reactor Theory*, Krieger Publishing, Malabar, Florida (1985).

[14] G.J. Habetler and B.J. Matkowsky, "Uniform Asymptotic Expansions in Transport Theory with Small Mean Free Paths, and the Diffusion Approximation," *J. Math. Phys.*, **16**, 846 (1975).

[15] M.G. Edwards, "Elimination of Adaptive Grid Interface Errors in the Discrete Cell Centered Pressure Equation," *J. Comp. Phys.*, **126**, 356 (1996).

[16] G.L. Olson and J.E. Morel, "Solution of the Radiation Diffusion Equation on an AMR Eulerian Mesh with Material Interfaces," LA–UR–99–2949, Los Alamos National Laboratory (1999).

[17] J.D. Densmore, "An Improved Method for Treating Monte Carlo-Diffusion Interfaces," *Trans. Am. Nucl. Soc.*, **91**, 139 (2004).

[18] J.D. Densmore, "Interface Methods for Hybrid Monte Carlo-Diffusion Radiation-Transport Simulations," *Ann. Nucl. Energy*, **33**, 343 (2006).

[19] G. Davidson, J.D. Densmore, A.K. Prinja, and J.E. Morel, "Asymptotically Correct Angular Distributions for Monte Carlo-Diffusion Interfaces," *Trans. Am. Nucl. Soc.*, **94**, 517 (2006).